# Stable Performance of Ni-Catalysts in Dry Reforming of Methane at High Temperatures for an Efficient CO_2-Conversion into Syngas**

Katharina Mette, Stefanie Kühl, Hendrik Düdder, Kevin Kähler, Andrey Tarasov, Martin Muhler,* Malte Behrens*

The efficient conversion of CO_2 into chemicals and fuels is a prospective building block for a more sustainable usage of our global resources [1]. Among the various strategies to convert CO_2 into higher-energy intermediates [2], heterogeneously catalyzed processes are of special interest, because they are scalable, based on a mature and flexible technology, which is already applied in chemical industries, and can be integrated into existing value chains [3]. The dry reforming of methane (DRM) with carbon dioxide is an interesting option to convert these two greenhouse gases into CO/H_2 mixtures (eq. 1). That opens the door to utilize anthropogenic CO_2, e.g. supplied from oxy-fuel combustion processes, in the well-established downstream syngas chemistry leading to methanol and other base chemicals or to fuels via Fischer-Tropsch synthesis.

(1) $CO_2 + CH_4 \rightarrow 2\ CO + 2\ H_2$ $\Delta H_{298} = 247$ kJ mol^{-1}
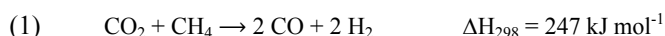
The highly endothermic DRM reaction has been studied since long time as a potential alternative for the steam reforming of methane and several comprehensive reviews are available [4,5,6]. It is well known that Ru, Rh or Pt catalysts are very active in this reaction. Active base metals, in particular Ni, suffer from fast deactivation by coking [7,8]. However, from an economical point of view Ni-based catalysts are more suitable for commercial application than noble metal ones. Thus, a current challenge is to find a noble metal-free catalyst that is resistant against coking [9]. Promising approaches reported in the literature include the poisoning of coke-forming sites by sulfur [10], variations of the supports [11], in particular application of Lewis-basic materials [12],

addition of some alkaline or earth-alkaline oxides as promoters [13,14,15], and incorporation of Ni in a perovskite framework [16].

It has been shown that carbon deposition over Ni at 700 °C and over Rh at 750 °C originates from the exothermic Boudouard reaction (eq. 2) and not primarily from methane decomposition (eq. 3) [17,18].

(2) $2\ CO \leftrightarrow CO_2 + C$ $\Delta H_{298} = $ -172 kJ mol^{-1}
(3) $CH_4 \rightarrow C + 2\ H_2$ $\Delta H_{298} = $ 75 kJ mol^{-1}

Thus, the process temperature is an important parameter of the DRM reaction [4]. Considering the thermodynamics of the desired endothermic DRM and the undesired exothermic Boudouard reactions, a promising way to suppress coking is to operate the DRM reaction at high temperatures [19]. Typically 750 °C is used as upper limit in many literature reports. In addition, the thermodynamic yield of CO and H_2 will increase at higher temperatures. Following this concept, the primary challenge of catalyst development of making the Ni particles kinetically more resistant against coking is enhanced by the goal of making a large Ni surface area thermally stable against sintering at even more elevated temperatures. Herein, we present the synthesis, characterization and catalytic performance of a Ni-rich bulk catalyst with sufficient thermal stability of its microstructure.

Our synthetic approach to stabilize Ni nanoparticles at high temperatures was to incorporate them into a stable oxide matrix – a concept previously applied for Ni-containing perovskites [16] and spinels [20]. We attempted to achieve strong interfacial interaction between metal and oxide with a stabilizing partial embedment of the Ni particles by formation of both catalyst components from a single phase precursor with a mixed cationic lattice and decomposable anions. This concept was previously applied for Cu-based catalysts for methanol synthesis, where Cu,Zn,Al hydrotalcites were developed as promising catalyst precursor materials [21]. The resulting catalysts are characterized by a homogeneous metal distribution and very small Cu particles that are embedded and therefore stabilized in an amorphous $ZnAl_2O_4$ matrix.

Following this concept, we have chosen a hydrotalcite-like (htl) precursor of the nominal composition $Ni_xMg_{0.67-x}Al_{0.33}(OH)_2(CO_3)_{0.17} \cdot m\ H_2O$, with x = 0.5. This precursor compound can be easily prepared in a phase-pure form by pH-controlled co-precipitation (see supporting information, SI, Fig. S1). Application of htl precursors for the preparation of Ni catalysts has been studied before by several groups for steam and dry reforming of methane. For instance, Takehira and co-workers [22-27] as well as Perez-Lopez et al. [28] presented different synthetic approaches to htl-derived $Ni/MgO/Al_2O_3$ catalysts, with Nickel contents ranging from 22 to 55 mol%, and investigated these materials in DRM. Moderate coking levels have been reported for a molar composition of Ni:Mg:Al of 55:11:33 between 500 and 700 °C. The high Ni content of 50 mol% (metal base) in our precursor corresponds to a 55 wt.-% Ni loading in the final catalyst. This rather high value was

[∗]   Katharina Mette, Dr. Stefanie Kühl, Dr. Andrey Tarasov, Dr. Malte Behrens
       Department of Inorganic Chemistry
       Fritz-Haber-Institut der Max-Planck-Gesellschaft
       Faradayweg 4-6, 14195 Berlin, Germany
       Fax: (+49) 030 8413 4405
       E-mail: behrens@fhi-berlin.mpg.de:

       Hendrik Düdder, Dr. Kevin Kähler, Prof. Dr. Martin Muhler
       Laboratory of Industrial Chemistry
       Ruhr-University Bochum
       Universtitätsstr. 150, 44801 Bochum
       Fax: (+49) 0234 32 14115
       E-mail: muhler@techem.rub.de

Supporting information for this article is available on the WWW under http://www.angewandte.org or from the author.

chosen to exploit the advantage of higher loadings of cheap and abundant base metal catalysts. The 1:2 ratio of Mg and Al is expected to lead to spinel formation, $MgAl_2O_4$, a sintering-stable ceramic compound. Furthermore, beneficial effects on the coking behavior of Ni catalysts have been reported on alumina, magnesia and spinel supports [29]. We will first focus on the synthesis and thermal stability of the htl-derived 55 wt.-% $Ni/MgAl_2O_4$ catalyst before the catalytic properties in DRM at high temperatures and the characterization of the spent samples will be reported.
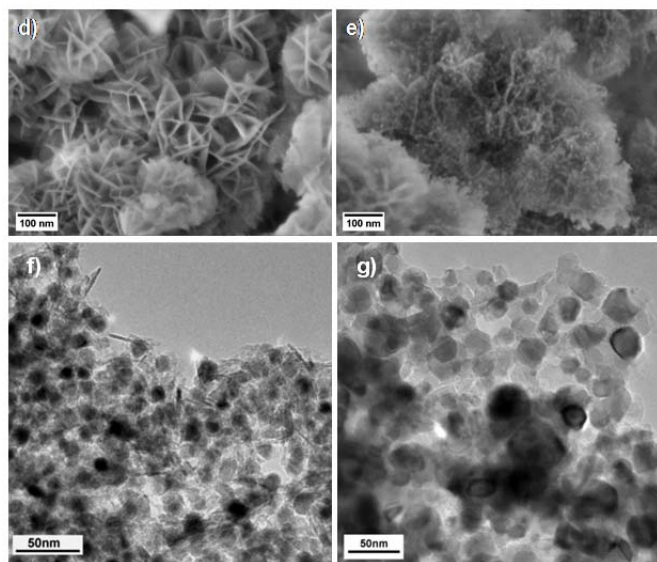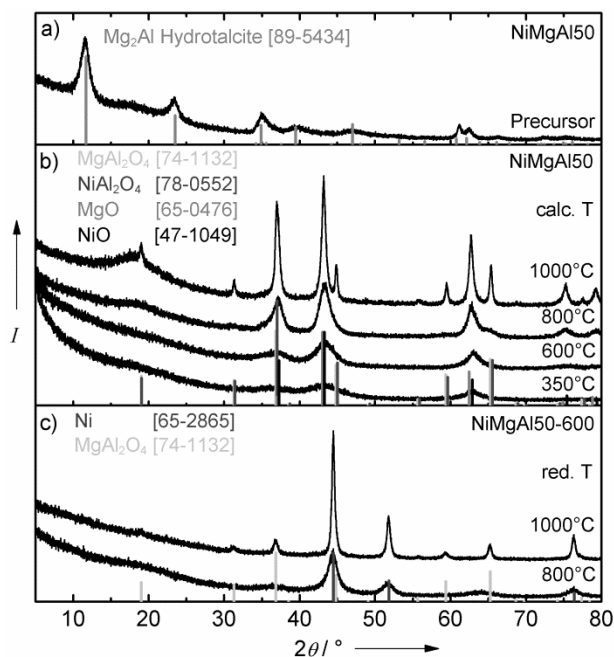

Figure 1. XRD patterns of the htl precursor (a), the calcination products obtained at different temperatures (b), the sample calcined at 600 °C after reduction at 800 and 1000 °C (c), SEM images of the precursor material (d) and the catalyst after reduction at 800 °C (e) and TEM micrographs of the fresh $Ni/MgAl_2O_4$ catalyst after reduction at 800 (f) and 1000 °C (g).

XRD analysis of the co-precipitated precursor confirmed the htl structure of the precursor and did not give any indication of other crystalline phases (Fig. 1a). In SEM, the typical platelet-like morphology of htl compounds can be observed with a lateral size of

up to approximately 200 nm and a thickness in the low nm range (Fig. 1d). The BET surface area of the precursor material was relatively high (131 $m^2 g^{-1}$). Upon calcination, the htl structure is decomposed and the precursor undergoes a weight loss of 38 % (measured up to 1000 °C), which is close to completion already at 600 °C (see SI for TGA curve, Fig. S2). The XRD patterns of the samples calcined at different temperatures are shown in Figure 1b. At 350 and 600 °C only broad modulations of the background are observed at the peak position of a rock salt structure-type phase (NiO or MgO). At 800 °C, crystallization has further progressed and first indications of a crystalline spinel phase are detected. After calcination at 1000 °C, the XRD pattern shows a mixture of a rock salt- and a spinel-type phase as expected for the decomposition product of a htl compound [30,31]. Due to the similar diffraction patterns of MgO and NiO and of $MgAl_2O_4$ and $NiAl_2O_4$ and the possible formation of solid solutions, no detailed phase identification can be achieved based on XRD, in particular for the poorly crystalline materials obtained at lower calcination temperatures. However, after mild calcination at 600 °C no indication for segregation of individual species was found by SEM and local EDX analyses at different locations (see SI, Fig. S3, Table S1). Thus, we conclude that the calcination product obtained at 600 °C is an amorphous, fully dehydrated and carbonate-free mixed Ni,Mg,Al oxide, whose homogenous distribution of the metal species has been largely conserved during decomposition of the htl precursor. The surface area has increased to 213 $m^2 g^{-1}$ due to the weight loss and shrinkage of the platelets.

After reduction of the calcined material in hydrogen at 800 °C (see SI for TPR curve, Fig. S4), SEM analysis revealed that the platelet-like morphology of the htl precursor is still present indicating a strong resistivity of the material against sintering at high temperatures (Fig 1e). In addition, small bright spheres can be observed in the micrograph homogeneously distributed over the platelets indicating that upon reduction a nanoscopic segregation of the components has taken place.

Indeed, XRD (Fig. 1c) clearly confirms the presence of metallic Ni after calcination at 600 °C and subsequent reduction at 800 °C with a domain size of 4 nm, according to a peak width analysis. The oxidic component is still only poorly crystalline and no sharp peaks of spinel can be detected. TEM analysis of individual platelets in the reduced material reveals an average particle size of Ni around 10 nm (Fig. 1f, SI Fig. S5). The discrepancy between XRD- and TEM-derived size data is thought to be caused by the polycrystalline and defect-rich nature of the embedded particles [32]. The Ni surface area was determined by hydrogen pulse chemisorption (SI, Fig. S6) and amounts to 22 $m^2 g_{cat}^{-1}$ at a BET surface area of 226 $m^2 g^{-1}$ after reduction. Interestingly, an increase of the reduction temperature to 900 °C did not significantly influence the Ni particle size (SI, Fig. S7). This is even more eminent since that temperature is far above the Tammann temperature of Nickel ($T_{Tammann, Ni}$= 581 °C [33]), proving the high thermal stability of this composite material. However, the domain size is increased to 7 nm, which is now in good agreement with the TEM analysis of around 9 nm (Table 1, SI Fig. S5), suggesting that the effect of temperature was rather an annealing of structural defects than sintering. Only treatment at 1000 °C leads to pronounced sintering of the Ni particles to an average Ni particle size around 19 nm according to TEM (Fig. 1g) and a domain size around 14 nm according to XRD. This process goes hand in hand with the beginning crystallization of the $MgAl_2O_4$ spinel in the oxide matrix (Fig. 1c). Accordingly, the specific Ni surface area was found to decrease only slightly to 88 % when

Table 1. Ni domain sizes and particle size distribution of NiMgAl50-600 after reduction at different temperatures.

T_{red} / °C	Domain size / nm[a]	Particle size / nm[b]	Particle size range / nm[b]	Ni surface area / m^2/g_{cat}[c]	Ni surface area / m^2/g_{Ni}[c]	Dispersion / %[d]	Interface ratio / %[e]
800	4.30 ± 0.20	10.4 ± 1.3	2 - 21	22	46	6.0	41.3
900	7.35 ± 0.11	8.9 ± 1.6	2 - 21	19	40	5.3	58.6
1000	14.10 ± 0.20	19.4 ± 2.2	7 - 44	6	12	1.6	67.8

[a] TOPAS fit LVol-IB [b] determined by TEM [c] determined by H_2 pulse chemisorption [d] calculated from H_2 pulse chemisorption measurements [e] calculated from Ni surface area and TEM particle size

increasing the reduction temperature from 800 to 900 °C and was breaking down to only 27 % at 1000 °C.

In summary, the characterization results show that the synthesis via the htl precursor yields a Ni catalyst that despite its high Ni loading of 55 wt.-% possesses a thermally stable microstructure up to 900 °C. This stability is probably due to the embedding nature of the still amorphous oxide matrix that separates the Ni nanoparticles from each other and therefore protects them from sintering, resulting in an interface-to-surface ratio of the particles of 41 % (see SI for detailed information). Even after thermal treatment up to 900 °C, the dispersion of the Ni particles (5-6%, Table 1) as well as the total specific surface area and the exposed specific Ni surface area is surprisingly high. Thus, these materials are promising catalysts that have the potential to withstand an increase of the reaction temperature of DRM to study the suppression of coking.
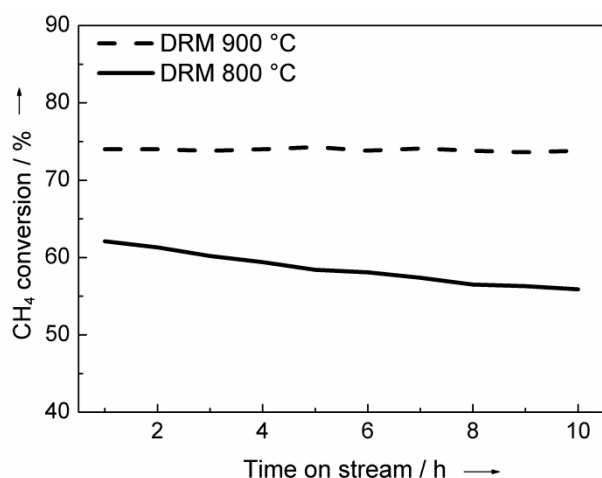
Figure 2. CH_4 conversion as a function of time on stream in the DRM at 800 °C and 900 °C using the Ni/MgAlOx catalyst after reduction up to 800 °C.

The catalytic activity and stability of the ex-htl catalysts was investigated in a fixed-bed reactor under isothermal DRM conditions. After a reductive pretreatment up to 800 °C the DRM reaction was performed at 800 °C and 900 °C. At the lower temperature a slight deactivation was observed, while during the DRM at 900 °C a higher and stable degree of conversion was detected (Fig. 2). Even in long-term experiments the catalyst showed a remarkable stable activity at 900 °C still achieving 94 % of the initial CH_4 conversion after 100 h (see SI, Fig. S8). This is attributed to the stabilizing effect of the oxide matrix that only allowed minor sintering of the active Ni nanoparticles as confirmed by TEM and XRD.

The integral rates of methane conversion, determined after 60 min time on stream are 3.5×10^{-3} mol s^{-1} g_{cat}^{-1} at 800 °C and 4.2×10^{-3} mol s^{-1} g_{cat}^{-1} at 900 °C. These are, to the best of our knowledge, the highest reported rates for DRM catalysts in literature.
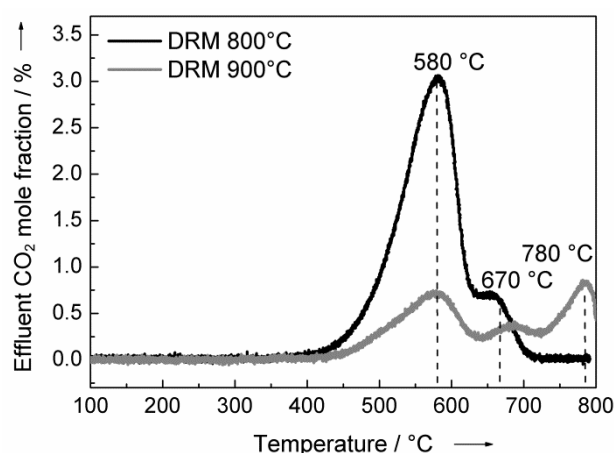
Figure 3. TPO profiles after DRM at 800 °C and 900 °C (F = 40 Nml min^{-1} 4.5 % O_2/Ar, β = 5 K min^{-1}, T_{max} = 800 °C) (Dry Reforming conditions: T_{Oven} = 800 °C or 900 °C, F_{total} = 240 Nml min^{-1} (32 % CH_4, 40 % CO_2, 28 % Ar (CO_2/CH_4 = 1.25))).

During a subsequent temperature-programmed oxidation (TPO) experiment the formation of CO_2 due to the presence of carbonaceous deposits was observed. In the TPO profile after DRM at 800 °C two signals at 580 °C and 670 °C were identified, which caused an overall amount of formed CO_2 of 117 mmol g_{cat}^{-1}. In DRM at 900 °C the carbon deposition was reduced to 54 mmol g_{cat}^{-1} including a third carbon species detected at 780 °C (Fig. 3). Once the carbon deposits were completely removed by TPO, the initial activity in DRM was recovered (see SI, Fig. S9). Thus, the observed deactivation during DRM at 800 °C was predominantly caused by the formation of carbon deposits and not by sintering. In agreement with the TPO results Raman spectra of spent samples after DRM revealed a lower graphitic content at 800 °C (SI, Fig. S12). These results indicate that the carbon formation mechanism is influenced by the reaction temperature. At 800 °C a significant amount of CNTs is formed giving rise to the TPO peak at 580 °C, whereas at 900 °C less CNTs and a more stable type of carbon are formed presumably from CH_4 by pyrolysis (eq. 3).

The presence of different amounts and types of carbon in the spent samples obtained were also seen in the TEM analysis of the catalysts run for 10 h in an analogous test, without a final TPO step. It was observed that after reaction at 800 °C in addition to a slight sintering of the Ni particles (SI, Fig. S10, Table S2) at least three

different carbon species were formed - carbon nanotubes (Fig. 4a), graphitic layers (Fig. 4c) and carbon onions with inclusions of Ni particles (Fig. 4b). TEM investigation of the catalyst run at 900 °C (SI, Fig. S11) confirmed the TPO result, as much less carbon was detected. Furthermore, CNTs are still present but to a much lower extent and less connected to the catalyst material.
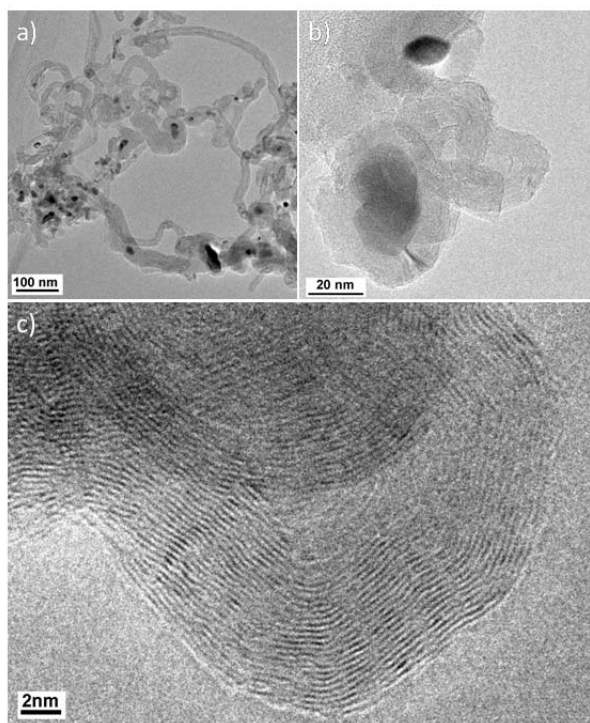

Figure 4. TEM micrographs of the spent sample run in DRM for 10 h at a reaction temperature of 800°C: a) CNT´s (containing Ni particles), b) isolated Ni particles in carbon onions and c) layers of graphitic carbon.

In summary, we have shown that mitigation of the coking problem of noble metal-free Ni catalyst for DRM is possible by elevating the operation temperature towards 900 °C. This favourable operational window can be exploited only if nanostructured catalysts with sufficient thermal stability are available to survive these harsh conditions. We reported the synthesis, characterization and catalytic testing of a highly active and stable Ni/MgAlO$_x$ catalyst that is characterized by small Ni particles, which are partially embedded in an oxide matrix with a high specific Ni and total BET surface area. Despite the high Ni loading of 55 wt.-%, this catalysts shows only minor sintering at 900 °C and performs stably in DRM over 100 hours with an outstandingly high rate of syngas formation. Compared to the lower reaction temperatures, the major problem of coking was to a large extent overcome on this stable Ni catalyst by an increase in reaction temperature to 900 °C, which leads to the formation of a less fibrous carbon.

Experimental Section

The catalysts were prepared by constant pH co-precipitation in an automated laboratory reactor (Mettler-Toledo Labmax) at 50 °C from aqueous 0.6 M NaOH, 0.09 M Na$_2$CO$_3$ solution and 0.4 M aqueous metal nitrate solution at pH 8.5. The obtained precursor was calcined in air at 600 °C for 3 h yielding almost amorphous mixed oxides.

For the catalytic experiments, 10 mg of the ex-htl Ni/MgAlOx catalyst (sieve fraction of 250-355 μm) prior calcined at 600 °C was used in a fixed-bed tubular quartz reactor. The sample was diluted in 490 mg SiC. For pretreatment, the catalyst was reduced in 20 Nml min^{-1} 4 % H$_2$/Ar. The DRM was performed at 800 or 900 °C in 240 Nml min^{-1} 40 % CO$_2$/32 % CH$_4$/Ar for 10, or 100 h, respectively. Subsequent TPO experiments were performed in 40 Nml min^{-1} 4.5 % O$_2$/Ar. Product gas analysis was performed using a multi-channel gas analyzer (MLT 4, Emerson) and a paramagnetic oxygen detector (Magnos 16, Hartmann & Braun) for transient experiments and a calibrated GC for the activity tests (Shimadzu GC-14B).
Further information to the experimental details is given in the SI.

[1]   C. Song, *Catal. Today* **2006**, 115, 2-32.
[2]   W. Wang, S. Wang, X. Ma, J. Gong, *Chem. Soc. Rev.* **2011**, 40, 3703-3727.
[3]   R. Schlögl, *ChemSusChem* **2010**, 3, 209-222.
[4]   M. C. J. Bradford, M. A. Vannice, *Catal. Rev.: Sci. Eng.* **1999**, 41, 1-42.
[5]   Y. H. Hu, E. Ruckenstein, *Adv. Catal.* **2004**, 48, 297-345.
[6]   M.-S. Fan, A. Z. Abdullah, S. Bhatia, *ChemCatChem* **2009**, 1, 192-208.
[7]   A. T. Ashcroft, A. K. Cheetham, M. L. H. Green, P. D. F. Vernon, *Nature* **1991**, 352, 225-226.
[8]   S. Wang, G. Q. Lu, *Energy & Fuels* **1996**, 10, 896-904.
[9]   C.-j. Liu, J. Ye, J. Jiang, Y. Pan, *ChemCatChem* **2011**, 3, 529-541.
[10]   J. R. Rostrup-Nielsen, *J. Catal.* **1984**, 85, 31-43.
[11]   M. C. J. Bradford, M. A. Vannice, *Appl. Catal. A* **1996**, 142, 73-96.
[12]   T. Horiuchi, K. Sakuma, T. Fukui, Y. Kubo, T. Osaki, T. Mori, *Appl. Catal. A* **1996**, 144, 111-120.
[13]   Z. L. Zhang, X. E. Verykios, *Catal. Today* **1994**, 21, 589-595.
[14]   S.-B. Tang, F.-L. Qiu, S.-J. Lu, *Catal. Today* **1995**, 24, 253-255.
[15]   T. Horiuchi, K. Sakuma, T. Fukui, Y. Kubo, T. Osaki, T. Mori, *Appl. Catal. A* **1996**, 144, 111-120.
[16]   V. R. Choudhary, B. S. Uphade, A. A. Belhekar, *J. Catal.* **1996**, 163, 312-318.
[17]   H. M. Swaan, V. C. H. Kroll, G. A. Martin, C. Mirodatos, *Catal. Today* **1994**, 21, 571-578.
[18]   V. A. Tsipouriari, A. M. Efstathiou, Z. L. Zhang, X. E. Verykios, *Catal. Today* **1994**, 21, 579-587.
[19]   J.-W. Snoeck, G. F. Froment, M. Fowles, *Ind. Eng. Chem. Res.* **2002**, 41, 4252-4265.
[20]   J. Guo, H. Lou, H. Zhao, D. Chai, X. Zheng, *Appl. Catal. A* **2004**, 273, 75-82.
[21]   a) M. Behrens, I. Kasatkin, S. Kühl, G. Weinberg, *Chem. Mater.* **2010**, 22, 386-397; b) S. Kühl, A. Tarasov, Stefan Zander, I. Kasatkin, M. Behrens, submitted to *Chem. Eur. J.* **2013**.
[22]   T. Shishido, M. Sukenobu, H. Morioka, R. Furukawa, H. Shirahase, K. Takehira, *Catal. Lett.* **2001**, 73, 21-26.
[23]   K. Takehira, T. Shishido, P. Wang, T. Kosaka, K. Takaki, *Phys. Chem. Chem. Phys.* **2003**, 5, 3801-3810.
[24]   K. Takehira, T. Shishido, P. Wang, T. Kosaka, K. Takaki, *J. Catal.* **2004**, 43-54.
[25]   A. I. Tsyganok, T. Tsunoda, S. Hamakawa, K. Suzuki, K. Takehira, T. Hayakawa, *J. Catal.* **2003**, 213, 191-203.
[26]   K. Takehira, T. Shishido, D. Shouro, K. Murakami, M. Honda, T. Kawabata, K. Takaki, *Appl. Catal., A* **2005**, 279, 41-51.
[27]   K. Takehira, T. Kawabata, T. Shishido, K. Murakami, T. Ohi, D. Shoro, M. Honda, K. Takaki, *J. Catal.* **2005**, 231, 92-104.
[28]   O. W. Perez-Lopez, A. Senger, N. R. Marcilio, M. A. Lansarin, *Appl. Catal. A* **2006**, 303, 234-244.
[29]   Y.-G. Chen, J. Ren, *Catal. Lett.* **1994**, 29, 39-48.
[30]   F. Cavani, F. Trifirò, A. Vaccari, *Catal. Today* **1991**, 11, 173-301.

[31] F. Zhang, X. Xiang, F. Li, X. Duan, *Catal. Surv. Asia* **2008**, 12, 253-265.

[32] J. Sehested, A. Carlsson, T. V. W. Janssens, P. L. Hansen, A. K. Datye, *J. Catal.* **2001**, 197, 200-209.

[33] J. Rostrup-Nielsen, L. J. Christiansen, in *Concepts in Syngas Manufacture*, Vol. 10 (Eds: G. J. Hutchings), Imperial College Press, London, **2011**, pp. 219-224.

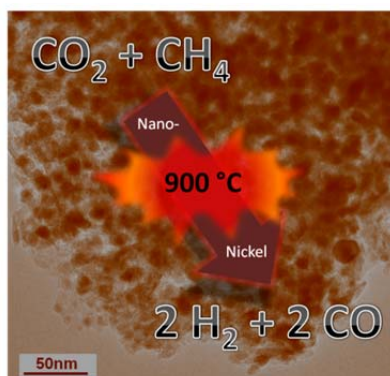**Entry for the Table of Contents** (Please choose one layout)

Layout 1:

Catalytic CO$_2$ Conversion

Katharina Mette, Stefanie Kühl, Hendrik Düdder, Kevin Kähler, Andrey Tarasov, Martin Muhler,* Malte Behrens*
_____ **Page – Page**

Stable Performance of Ni-Catalysts in Dry Reforming of Methane at High Temperatures for an Efficient CO$_2$-Conversion into Syngas

A thermally outstandingly stable Nickel-based catalyst is presented that maintains small Ni nanoparticles of a size around 10 nm even at a temperature of 900 °C. This material allows elevation of the operation temperature of the dry reforming of methane to convert the green house gases CO$_2$ and CH$_4$ into useful syngas into a regime, where coking is largely mitigated without addition of noble metals.